

# The C2 domains of dysferlin: roles in membrane localization, Ca<sup>2+</sup> signalling and sarcolemmal repair

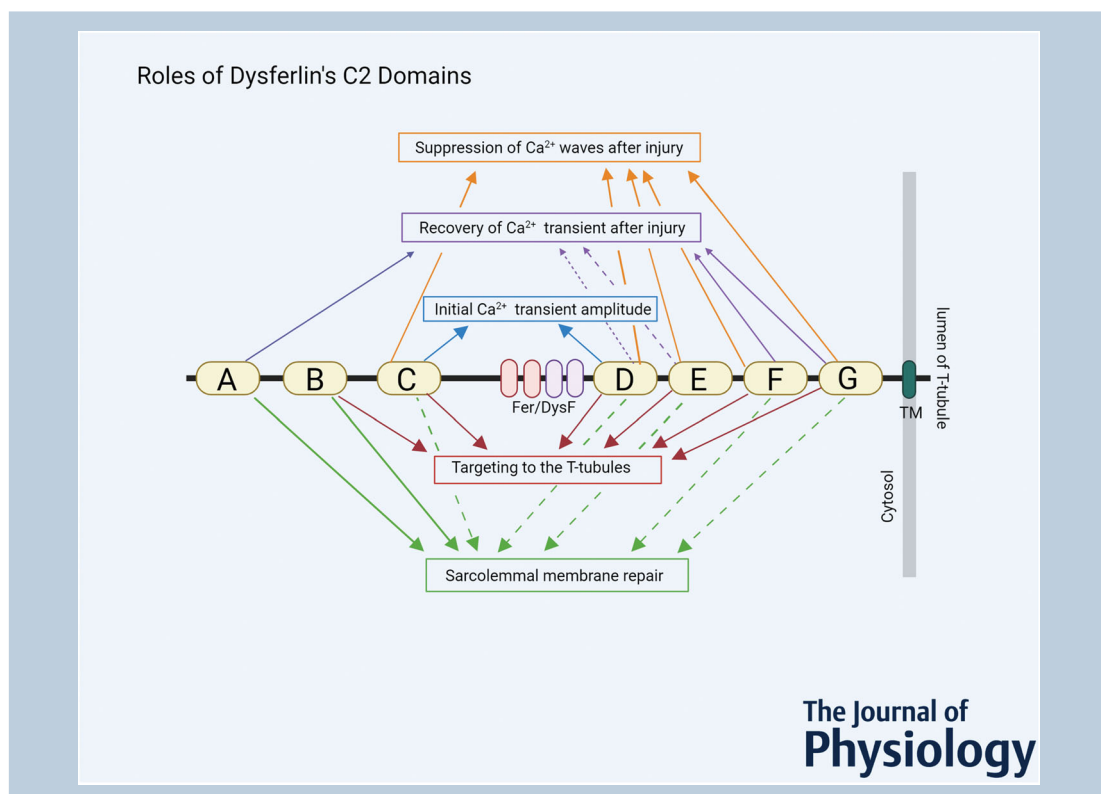
Joaquin Muriel<sup>1</sup>, Valeriy Lukyanenko<sup>1</sup> , Tom Kwiatkowski<sup>2</sup>, Sayak Bhattacharya<sup>2</sup>, Daniel Garman<sup>1</sup> , Noah Weisleder<sup>2</sup> and Robert J. Bloch<sup>1</sup> 

<sup>1</sup>Department of Physiology, University of Maryland School of Medicine, Baltimore, MD, USA

<sup>2</sup>Department of Physiology and Cell Biology, Dorothy M. Davis Heart and Lung Research Institute, The Ohio State College of Medicine, Columbus, OH, USA

Edited by: Peking Fong & Nordine Helassa

The peer review history is available in the Supporting Information section of this article (<https://doi.org/10.1113/JP282648#support-information-section>).



**Robert J. Bloch** received his AB degree from Columbia University (New York, NY) and his PhD from Harvard University (Cambridge, MA), where he studied with Dr Guido Guidotti. He subsequently did postdoctoral research with Dr Max M. Burger at the Biozentrum, University of Basel, Switzerland, and Dr Stephen Heinemann, at the Salk Institute, La Jolla, CA. He has been a member of the faculty of the Physiology Department, University of Maryland School of Medicine, since 1980. His research focuses on the biology of skeletal muscle and how genetic and epigenetic changes lead to muscular dystrophies.



J. Muriel and V. Lukyanenko contributed equally to this work.

**Abstract** Dysferlin is an integral membrane protein of the transverse tubules of skeletal muscle that is mutated or absent in limb girdle muscular dystrophy 2B and Miyoshi myopathy. Here we examine the role of dysferlin's seven C2 domains, C2A through C2G, in membrane repair and  $\text{Ca}^{2+}$  release, as well as in targeting dysferlin to the transverse tubules of skeletal muscle. We report that deletion of either domain C2A or C2B inhibits membrane repair completely, whereas deletion of C2C, C2D, C2E, C2F or C2G causes partial loss of membrane repair that is exacerbated in the absence of extracellular  $\text{Ca}^{2+}$ . Deletion of C2C, C2D, C2E, C2F or C2G also causes significant changes in  $\text{Ca}^{2+}$  release, measured as the amplitude of the  $\text{Ca}^{2+}$  transient before or after hypo-osmotic shock and the appearance of  $\text{Ca}^{2+}$  waves. Most deletants accumulate in endoplasmic reticulum. Only the C2A domain can be deleted without affecting dysferlin trafficking to transverse tubules, but Dysf- $\Delta$ C2A fails to support normal  $\text{Ca}^{2+}$  signalling after hypo-osmotic shock. Our data suggest that (i) every C2 domain contributes to repair; (ii) all C2 domains except C2B regulate  $\text{Ca}^{2+}$  signalling; (iii) transverse tubule localization is insufficient for normal  $\text{Ca}^{2+}$  signalling; and (iv)  $\text{Ca}^{2+}$  dependence of repair is mediated by C2C through C2G. Thus, dysferlin's C2 domains have distinct functions in  $\text{Ca}^{2+}$  signalling and sarcolemmal membrane repair and may play distinct roles in skeletal muscle.

(Received 23 November 2021; accepted after revision 3 February 2022; first published online 14 February 2022)

**Corresponding authors** R. J. Bloch: Department of Physiology, University of Maryland School of Medicine, 655 W. Baltimore St., Baltimore, MD 21208, USA. Email: rbloch@som.umaryland.edu

N. Weisleder: Department of Physiology and Cell Biology, Dorothy M. Davis Heart and Lung Research Institute, The Ohio State University Wexner Medical Center, 473 W. 12th Avenue, Columbus, OH 43210-1252, USA. Email: noah.weisleder@osumc.edu

**Abstract figure legend** The C2 domains of dysferlin play different roles in 5 different activities of the protein: targeting to the transverse tubules, supporting membrane repair, supporting the amplitude of the  $\text{Ca}^{2+}$  transient, supporting the amplitude of the  $\text{Ca}^{2+}$  transient after injury by hypoosmotic shock (OSI), and suppressing  $\text{Ca}^{2+}$  waves after OSI. The relative contributions of each domain to these activities are indicated here. Solid lines: notable contribution; dashed lines, moderate contribution; dotted lines, minimal contribution. The absence of a line indicates that no contribution was detected.

### Key points

- Dysferlin, a transmembrane protein containing seven C2 domains, C2A through C2G, concentrates in transverse tubules of skeletal muscle, where it stabilizes voltage-induced  $\text{Ca}^{2+}$  transients and participates in sarcolemmal membrane repair.
- Each of dysferlin's C2 domains except C2B regulate  $\text{Ca}^{2+}$  signalling.
- Localization of dysferlin variants to the transverse tubules is not sufficient to support normal  $\text{Ca}^{2+}$  signalling or membrane repair.
- Each of dysferlin's C2 domains contributes to sarcolemmal membrane repair.
- The  $\text{Ca}^{2+}$  dependence of membrane repair is mediated by C2C through C2G.
- Dysferlin's C2 domains therefore have distinct functions in  $\text{Ca}^{2+}$  signalling and sarcolemmal membrane repair.

### Introduction

Dysferlin is a 237 kDa integral membrane protein that is mutated or absent in limb girdle muscular dystrophy type 2B (LGMD2B) and Miyoshi myopathy (MMD1) (reviewed in Urtizbera *et al.* 2008; Amato & Brown, 2011; Patel *et al.* 2017), as well as other, rarer myopathies. Most of the protein faces the cytoplasm and contains seven C2 domains, C2A through C2G, with additional ferlin-like domains, Fer and DysF, sandwiched between the C2 domains in the middle of the molecule,

between C2C and C2D (reviewed in Lek *et al.* 2012). Each of the C2 domains can bind  $\text{Ca}^{2+}$  and lipid, though with widely varying affinities (Davis *et al.* 2002; Therrien *et al.* 2009; Marty *et al.* 2013; Abdullah *et al.* 2014; Fuson *et al.* 2014; Golbek *et al.* 2021; Wang *et al.* 2021). The more N-terminal C2 domains are involved in forming multi-protein complexes with ligands such as AHNAK and TRIM72/MG53 (Huang *et al.* 2007; Matsuda *et al.* 2012), but the binding sites of several other protein ligands, including the dihydropyridine receptor,

caveolin 3 and SNARES (Matsuda *et al.* 2001; Lennon *et al.* 2003; Ampong *et al.* 2005; Hernández-Deviez *et al.* 2006; Cai *et al.* 2009b; de Morrée *et al.* 2010; Coddling *et al.* 2016) have not yet been identified. The protein is anchored to membranes by a transmembrane sequence near its C-terminus. In other cell types and tissues, dysferlin associates with the plasma membrane and with membrane-bound vesicles involved in exocytosis or endocytosis (Anderson *et al.* 1999; McNeil *et al.* 2000; Jethwaney *et al.* 2007; Han *et al.* 2012; Davenport & Bement, 2016), but in skeletal muscle it concentrates in the transverse tubules (TT; Ampong *et al.* 2005; Klinge *et al.* 2007; Roche *et al.* 2011; Kerr *et al.* 2013; Lukyanenko *et al.* 2017). Remarkably, despite years of study, the role of dysferlin in skeletal muscle is still unclear. Two contrasting though not mutually exclusive roles have been proposed: mediating membrane repair and stabilizing  $\text{Ca}^{2+}$  signalling. Both have considerable experimental support.

The earliest studies of dysferlin-null muscles in mice and man suggested a role in sarcolemmal membrane repair (Bansal *et al.* 2003; Lennon *et al.* 2003; reviewed in Bansal & Campbell, 2004; Glover & Brown, 2007; Han & Campbell, 2007). Consistent with this, muscle fibres or fibre bundles that were injured either by laser ablation or needle puncture resealed their plasma membranes less rapidly when dysferlin was absent than in wild-type controls, as assayed by uptake of a lipophilic dye. Dysferlin-null muscle also showed an accumulation of vesicles near the sarcolemma, suggesting a defect in their ability to fuse (Piccolo *et al.* 2000; Selden *et al.* 2001; Bansal *et al.* 2003; Cenacchi *et al.* 2005). This would be consistent with dysferlin's putative role in membrane fusion in other tissues. Subsequent studies identified several dysferlin-associated proteins that are themselves linked to membrane repair and stability, including TRIM72/MG53, annexins and caveolin 3 (Cav3) (Matsuda *et al.* 2001; Lennon *et al.* 2003; Hernández-Deviez *et al.* 2006; Cai *et al.* 2009b; de Morrée *et al.* 2010; Waddell *et al.* 2011; Matsuda *et al.* 2012; Carmeille *et al.* 2016; Coddling *et al.* 2016; Demonbreun *et al.* 2016). Most recently, dysferlin was shown to incorporate into the repair patch together with other proteins of the TT, after incorporation of annexins and in an actin-dependent process (McDade *et al.* 2014; Demonbreun *et al.* 2016). Immunolocalization of dysferlin in several of these studies suggested that it concentrates at the sarcolemma of skeletal muscle, in vesicle-like structures in the myoplasm, and, after injury, in membrane repair patches (Bansal *et al.* 2003; Cai *et al.* 2009a; Weisleder *et al.* 2009).

Other studies have questioned whether dysferlin is essential for sarcolemmal repair and suggested that it might support other essential activities in muscle. Murine muscle fibres lacking dysferlin resealed like wild-type

fibres after an *in vivo* injury caused by large strain lengthening contractions (Roche *et al.* 2008; Roche *et al.* 2010). The major difference between dysferlin-positive and dysferlin-negative muscle only appeared many hours after injury and resealing, when the former recovered from injury while the latter underwent necrosis and recovered function following fibre regeneration (Roche *et al.* 2010). Furthermore, immunolabelling studies with fibres that were prefixed *in situ* prior to labelling and treated with mild acid to expose dysferlin epitopes showed most of the dysferlin in wild-type muscle to be at or near the triad junctions of skeletal muscle, with very little at the sarcolemma (Roche *et al.* 2011). The accumulation of dysferlin in TT was clearly demonstrated in studies of fibres transfected with dysferlin-pHluorin, which accumulated at or near triad junctions and lost its fluorescence upon exposure to solutions of low pH, indicating that the C-terminus of dysferlin linked to pHluorin was exposed to the extracellular milieu, which can access the lumen of the TT (Kerr *et al.* 2013; McDade *et al.* 2014; Lukyanenko *et al.* 2017). These studies also showed that dysferlin's absence is associated with a small decrease in the amplitude of voltage-induced  $\text{Ca}^{2+}$  transients (Kerr *et al.* 2013; Lukyanenko *et al.* 2017), suggesting that dysferlin is required for optimal coupling between the L-type  $\text{Ca}^{2+}$  channel (LTCC) and the ryanodine receptor (RyR1) at the triad junction. Dysferlin-null fibres also show increased susceptibility to injury by a mild hypo-osmotic shock *in vitro* that increases cytoplasmic  $\text{Ca}^{2+}$  levels and diminishes the amplitude of the  $\text{Ca}^{2+}$  transient, accompanied by the spontaneous generation of  $\text{Ca}^{2+}$  sparks and waves (Kerr *et al.* 2013; Lukyanenko *et al.* 2017). These changes are all blocked by inhibitors of the voltage-gated  $\text{Ca}^{2+}$  channel (dihydropyridine receptor) and the sarcoplasmic reticulum  $\text{Ca}^{2+}$  release channel (ryanodine receptor 1) (Lukyanenko *et al.* 2017). Notably,  $\text{Ca}^{2+}$  sparks and waves are indicative of  $\text{Ca}^{2+}$ -induced  $\text{Ca}^{2+}$  release (CICR), which is thought to be pathogenic in mammalian skeletal muscle (Endo 2009; Ríos 2018). This suggests that dysferlin is required to stabilize the  $\text{Ca}^{2+}$  release events that underlie excitation-contraction coupling in skeletal muscle (see Kerr *et al.* 2014).

We have begun a comprehensive study of structure-function relationships in dysferlin with the goal of defining the role of its different structural domains in maintaining the health of skeletal muscle. We hypothesized that the defect in  $\text{Ca}^{2+}$  handling in dysferlin-null muscle was the primary pathogenic factor and that defects in sarcolemmal membrane repair were secondary. We reasoned that if this is true, then every mutation in dysferlin that dysregulates  $\text{Ca}^{2+}$  would also affect membrane repair. Here we report the effects of deleting each of dysferlin's C2 domains on its ability to localize to the TT membrane, support sarcolemmal membrane repair and stabilize  $\text{Ca}^{2+}$  handling in the myocyte. Our

results show that the C2 domains of dysferlin have distinctive roles in these processes and suggest that stabilization of  $\text{Ca}^{2+}$  release and support of membrane repair are at least in part independent processes. These results have significant implications for our understanding of the molecular function of dysferlin and the treatment of dysferlinopathy.

## Methods

### Ethical approval

All procedures were approved by the Institutional Animal Care and Use Committees of the University of Maryland, Baltimore, and the Ohio State University according to federal guidelines (institutional animal welfare assurance numbers A3200-01 and A3261-01, respectively). All co-authors understand the ethical principles under which *The Journal of Physiology* operates and confirm that their work complies with its guidelines for the ethical use of animals in research.

Male A/J mice were from The Jackson Laboratory (Bar Harbor, ME, USA). (Only males were used for these studies, as they respond more reproducibly to injury.) They were studied at 3 months of age, when their weights were approximately 27 g. Mice were maintained on normal chow with *ad libitum* access to food and water. Anaesthesia prior to intramuscular injections used 3–4.5% isoflurane in oxygen. Carprofen (5 mg/kg) was administered subcutaneously prior to injections performed at the University of Maryland, Baltimore. Post-injection, mice were monitored to ensure their recovery from anaesthesia, then daily for 3 days thereafter. Subsequent monitoring was 3 times per week. Anaesthesia prior to euthanasia used >4.5% isoflurane in oxygen, after which mice were euthanized by bilateral thoracotomy. All *in vitro* experiments were performed at room temperature.

The number of mice used for localization of the dysferlin variants ranged from three to six and for sarcolemmal membrane repair from three to five. The number used for studies of  $\text{Ca}^{2+}$  signalling ranged from 5 to 13 mice per dysferlin variant, 17 mice transfected to express Venus linked to wild-type dysferlin, and seven transfected to express Venus alone. A total of 162 mice were used. No animals were excluded.

### Electroporation of flexor digitorum brevis

Electroporation of flexor digitorum brevis (FDB) muscles for measurements of  $\text{Ca}^{2+}$  signalling (Kerr *et al.* 2013; Lukyanenko *et al.* 2017) and of membrane repair (Zhao *et al.* 2012) followed the methods of DiFranco *et al.* (2009). All dysferlin variants contained an N-terminal Venus fluorescence tag to identify transfected muscle fibres. Fibres were cultured by removing FDB muscles 9–13 days

after electroporation and digesting them with collagenase prior to culturing them on a Matrigel (Sigma-Aldrich, St Louis, MO, USA) surface. Experiments were performed 1–2 days later.

### cDNA constructs

cDNA constructs were prepared in the pcDNA vector and expressed under the control of the CMV promoter. Oligonucleotides used in the PCR to generate the various dysferlin variants and the amino acids deleted to remove one or more of its C2 domains are given in Table 1. Deletions were engineered as follows. Reverse primers were annealed with the sequence immediately upstream to the deletion. Forward primers were annealed with the sequence immediately downstream to the deletion. The 5' ends of the forward primers were tailed with the sequence immediately upstream to the deletion. Plasmid with full length dysferlin was used as a template. All variants were expressed as N-terminal Venus fusion proteins, for studies of  $\text{Ca}^{2+}$  signalling or membrane repair. C-terminal fusions with pHluorin were used to assess localization to TT, as described (Lukyanenko *et al.* 2017).

### Transfection

Transfection of HEK293 cells was as described (Weisleder *et al.* 2012). Transfection of FDB muscles was by electroporation, as reported (Zhao *et al.* 2012; Kerr *et al.* 2013; Lukyanenko *et al.* 2017). At 1–2 weeks after electroporation, muscles were removed and either dissociated and cultured for studies of  $\text{Ca}^{2+}$  signalling and TT localization, or teased into small bundles for studies of membrane repair.

### Immunolabelling for desmin

Immunolabelling for desmin used polyclonal rabbit antibodies to desmin and Alexa 568-conjugated goat anti-rabbit IgG, as described (Sakellariou *et al.* 2016). In brief, fibres were fixed with 2% paraformaldehyde in phosphate-buffered saline (PBS) for 15 min, permeabilized with 0.25% Triton X-100 in PBS, incubated for an hour or more at room temperature in 3% BSA, 0.01% Triton X-100 in PBS. The BSA–Triton solution was also used to dilute the primary antibodies.

### $\text{Ca}^{2+}$ release

$\text{Ca}^{2+}$  release events were assayed as described (Lukyanenko *et al.* 2017). Briefly, isolated FDB fibres were loaded with 4.45  $\mu\text{M}$  Rhod-2AM (Thermo Fisher Scientific, Waltham, MA, USA) for 45 min at 37°C. Trains of voltage-induced  $\text{Ca}^{2+}$  transients were induced by field stimulation (1 Hz for 10 s) every 1 min. Rhod-2 was visualized with a Zeiss Duo confocal microscope

(Carl Zeiss Microscopy, Oberkochen, Germany). Fluorescence was excited with 560 nm laser light and emitted light was measured at wavelengths of  $>575$  nm, set with a LP 575 filter. Line scan images were acquired in the middle of myofibres at a rate of 1.9 ms/line with the aperture of the confocal detector set to maximum. We used ImageJ 1.31v (NIH, Bethesda, MD, USA) to determine the mean maximal value of the  $\text{Ca}^{2+}$  transients. The values reported were measured as the difference between maximal fluorescence intensity ( $F_{\text{max}}$ ) and background fluorescence ( $F_0$ ), normalized to  $F_0$ . For mild osmotic shock injury, cultured FDB fibres were superfused for 1 min with a hypotonic Tyrode solution with the concentration of NaCl reduced to 70 mM. Cells were then superfused with isotonic Tyrode solution for 5 min. Experiments were performed at room temperature (21–23°C).

### Levels of transfection

Levels of transfection were evaluated by assessing the Venus fluorescence in each myofibre before imaging Rhod-2 fluorescence. The confocal diaphragm was set at 1 Airy unit, the intensity of the 488 nm laser was reduced to 1%, and the gain was adjusted to obtain an average cell autofluorescence in the Venus channel of 200 arbitrary units (AU; maximum = 4095 AU), measured in untransfected cells that lacked a Venus signal. Venus fluorescence intensity was measured from 100 pixels per cell with ImageJ 1.31v (NIH, Bethesda, MD).

### Membrane repair

Membrane repair was assayed as reported (Gushchina *et al.* 2017). Briefly, FDB muscles were surgically isolated and placed in  $\text{Ca}^{2+}$ -free Tyrode solution (140 mM NaCl, 5 mM KCl, 2 mM  $\text{MgCl}_2$ , 10 mM HEPES, pH 7.2). Muscle bundles were mechanically separated at the tendon and

then adhered on glass-bottomed culture dishes (MatTek, Ashland, MA, USA) with Liquid Bandage (New Skin, Tarrytown, NY, USA) applied to the exposed tendons. Membrane disruption was induced in Tyrode solution supplemented with 2.5  $\mu\text{M}$  FM 4–64 dye (Thermo Fisher Scientific), and in either 2 mM  $\text{Ca}^{2+}$  or 2 mM EGTA, with a FluoView FV1000 multi-photon confocal laser-scanning microscope (Olympus, Center Valley, PA, USA). A 2.5  $\mu\text{m}$  circular region of interest was selected along the edge of the sarcolemma and irradiated at 10% of maximum infrared laser power for 3 s. Images were captured before and after damage, every 5 s for a total of 60 s. Images were analysed with ImageJ Fiji, by measuring the fluorescence intensity encompassing the site of damage, with results represented as  $\Delta F/F_0$ . The area under the curve and the peak FM4-64 intensity were calculated with GraphPad Prism software (GraphPad Software, La Jolla, CA, USA).

### Statistics

Statistics were analysed with Prism or SigmaPlot 13.0 (Systat Software, Inc., San Jose, CA, USA) software, with  $P < 0.05$  considered significant. All data were collected from muscles or myofibres from three or more mice and are displayed as mean  $\pm$  SD.

### Materials

Materials were obtained from Sigma-Aldrich (St Louis, MO, USA) and Thermo Fisher Scientific unless otherwise noted.

### Results

We used PCR-based methods to create dysferlin variants missing each of the C2 domains, A through G, and one construct of ‘minidysferlin’ containing only C2 domains A and G (Dysf- $\Delta\text{B-F}$ ; see Fig. 1A and Table 1). Each

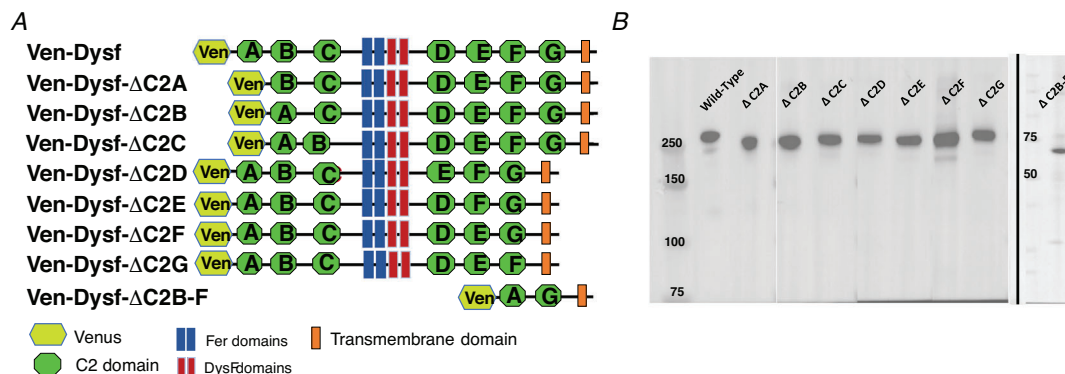


**Figure 1. The C2 deletion constructs studied**

A, cartoon depicting the constructs. Not to scale. B, SDS-PAGE and western blot analysis of the deletion mutants pictured in A. Samples were from HEK293 cells transfected with each of the deletants, then extracted, analysed by SDS-PAGE and immunoblotted with Hamlet antibodies to dysferlin.

Table 1. Sequences of oligonucleotides used to create deletion mutations of dysferlin

Deletion mutation	Amino acids deleted	Forward primer	Reverse primer
Dysf- $\Delta$ C2A	2–190**	<b>GT</b> TAAACGATCGGCCGCCACC <u>AT</u> GCACGTCCTCCGCCCACTAC**	CATGGTGGCGGCCGATCGTTTAAAC
Dysf- $\Delta$ C2B	131–349*	<b>CT</b> ACACCCGCTGCTGGAGCTGGCGCTCTGGAGAGAAAAGAC	CACAGCTCAGGCAGCGGTGTGTAG
Dysf- $\Delta$ C2C	348–524	<b>CT</b> TTGTGCTGGGGCTGGGCTATGGCAGTCCAGAGAGTTC	CCAGGCCAGCACAAAG
Dysf- $\Delta$ C2D	1132–1307	<b>G</b> AGTGAAGATCCATGCTCCCTCCCTACCCACCACCCAGAG	GGAGAGGACATGGAATCTTCACTC
Dysf- $\Delta$ C2E	1291–1537	<b>CA</b> TCCACATATTCGTTGGAGGATCCATCTGATTGGTGAATTAAG	CTCAAAACCAGGAATATGGTGGATG
Dysf- $\Delta$ C2F	1468–1781	<b>CA</b> TTGATGACAAAGAGCCCTCATCAAGCTGCAGATGGGTGCGACTATTC	GATGAGGGGCTCTTGTCAATAATG
Dysf- $\Delta$ C2G	1709–1971	<b>CA</b> GTCTCCACCTCTTCGCCAGCAGTAGCAGAAAGGGGTGAGAAGAAAATAC	CTGTGGCAGAAGAGGTGGAGGAGCTG
Dysf- $\Delta$ C2B–F	131–1781	<b>CT</b> ACACCCGCTCGGAGCTGGAAGCTGCAGATGGGGTGCACCTATTC	CACAGCTCAGGCAGCGGTGTGTAG

Sequences in bold indicate sequences complementary to the reverse primer.

\* Deletions also remove the linker region between C2A and C2B.

\*\* Underlined = start codon.

variant was tagged at its N-terminus with Venus or at its C-terminus with pHluorin. With the exception of Dysf- $\Delta$ B–F, which expressed poorly, all of these constructs expressed well in HEK293 cells, with no evidence of degradation as assayed by immunoblotting with antibodies to dysferlin (Fig. 1B). All variants lacking individual C2 domains had an apparent molecular mass of  $\sim$ 250–260 kDa, equivalent to the sum of the masses of the Venus moiety and the truncated dysferlin molecule, and could also be labelled in blots with antibodies to green fluorescent protein, confirming the identity of the fusion proteins (not shown). Venus–Dysf- $\Delta$ B–F expressed in HEK293 cells had the expected molecular mass in SDS-PAGE gels of  $\sim$ 70 kDa (Fig. 1B).

### Subcellular localization

We introduced the fluorescent dysferlin variants into muscle fibres of the flexor digitorum brevis (FDB) muscles of dysferlin-null A/J mice by electroporation (Kerr *et al.* 2013; Lukyanenko *et al.* 2017). Two weeks later we removed the muscles, dissociated the fibres by enzymatic digestion and placed them in culture. We first determined the localization of each construct under fluorescence optics alone (Figs 2A and C) and after colabelling for the sarcomeric marker desmin, which labels at the level of the Z-disk (Fig. 2B). In these assays, Venus and pHluorin constructs of WT-dysferlin label at the level of the A–I junctions, where they concentrate in the TT, which appear as double lines of punctate structures within each sarcomere (Kerr *et al.* 2013; Lukyanenko *et al.* 2017). All of the deletion constructs, with the exception of Venus–Dysf- $\Delta$ C2A, and to lesser extents - $\Delta$ C2B and - $\Delta$ C2C, showed little or no presence in the puncta at the level of A–I junctions but instead concentrated in short linear structures, parallel to the long axis of the fibre, centred at the Z-disk and extending towards the A–I junctions nearby. We obtained the same result with Venus–Dysf- $\Delta$ C2B–F. A DS-Red construct with a KDEL endoplasmic reticulum (ER) retention sequence concentrated in similar longitudinal structures, suggesting that this membrane compartment comprises part of the ER (Fig. 2A, lower right panel). These results suggest that C2 domains D through G are all necessary for the Venus-tagged protein to target membranes at the level of the A–I junctions of murine myofibres and that in their absence their default location is the ER.

We used C-terminal pHluorin constructs of the dysferlin variants to quantify their ability to target the membranes of the TT. As reported, the fluorescence of WT-Dysf-pHluorin changes substantially in response to decreases in extracellular pH, indicative of TT localization (Kerr *et al.* 2013; Lukyanenko *et al.* 2017). None of the pHluorin constructs of the domain deletion variants do so, however (Fig. 3), with the exception of

Dysf-ΔC2A-pHluorin. These results suggest that all of its C2 domains except C2A are required for dysferlin to concentrate in TT. Notably, although Venus-Dysf-ΔC2B and to a lesser extent Venus-Dysf-ΔC2C concentrate in puncta at the A-I junction as N-terminal Venus and as C-terminal pHluorin constructs (Fig. 2), neither construct responds to changes in extracellular pH, suggesting

that the two do not concentrate in TT, with their C-termini exposed to the TT lumen, like WT dysferlin or Dysf-ΔC2A (Fig. 3). Consistent with its localization in the same compartment as many of the dysferlin variants, KDEL-pHluorin failed to show a significant change in fluorescence in response to decreases in extracellular pH (not shown).

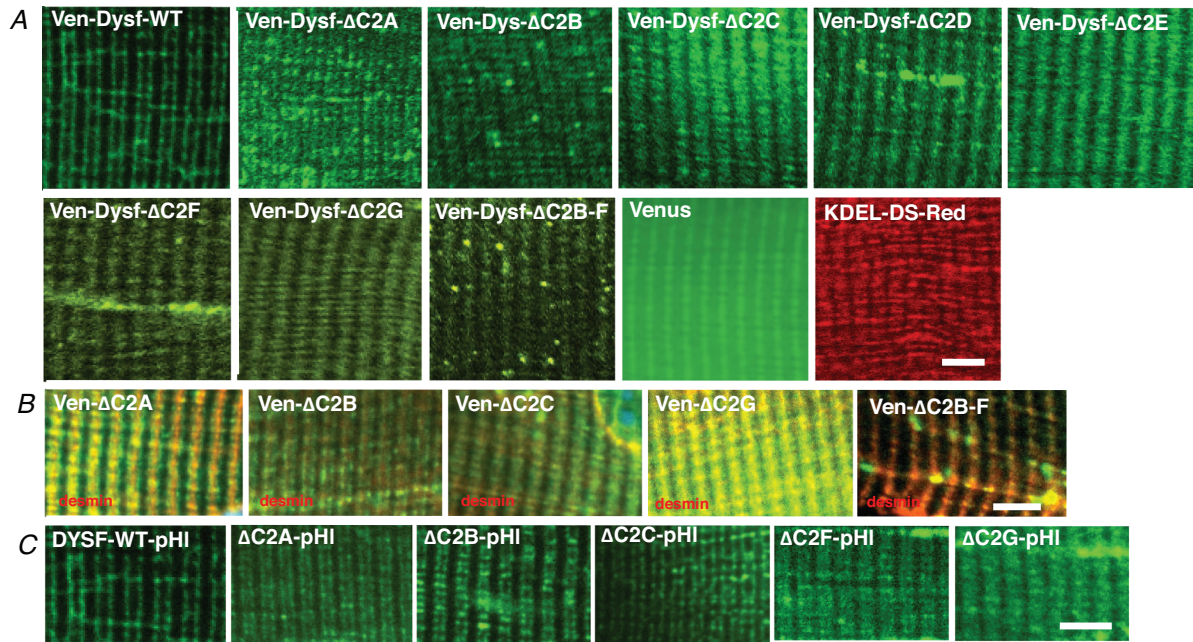
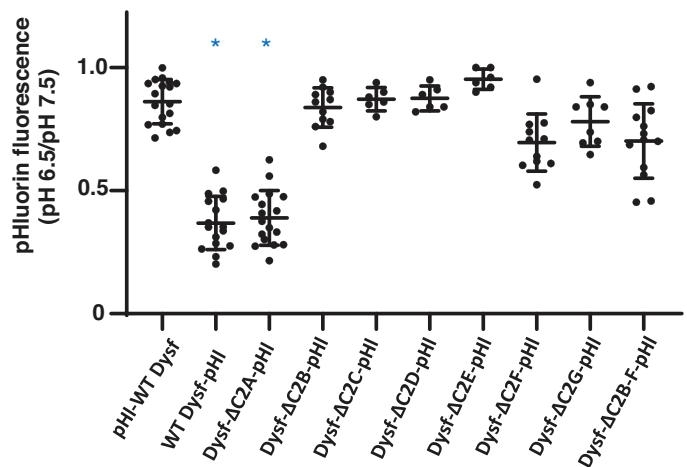


**Figure 2. Distribution of the C2 deletion constructs in FDB myofibres and comparison to desmin**  
 FDB muscles were electroporated in the presence of 1.2 μg DNA encoding each of the C2 deletion constructs, created as N-terminal Venus constructs (A and B) and as C-terminal pHluorin constructs (C), both shown in green as well as with KDEL-DS-Red (A, lower right panel, shown in red). Two weeks later, fibres were isolated, placed in culture for 24 h and then imaged for Venus, pHluorin or DS-Red under confocal optics (A and C). Alternatively, they were fixed, permeabilized and immunolabelled for desmin followed by anti-antibodies coupled to Alexa Fluor 568 (B, shown in red). Note that not all constructs are shown in B and C; rather, ΔC2D, ΔC2E and ΔC2F give identical patterns to ΔC2G in set B, and ΔC2D, ΔC2E and ΔC2B-F give identical patterns to ΔC2G in set C. The scale bars in the lower right panels represent 5 μm and apply to all panels in each set.

**Figure 3. Changes in fluorescence of C2 domain deletants with C-terminal pHluorin**

FDB muscles were studied as in Fig. 2 after transfection with C-terminal pHluorin constructs of each of the deletion mutants as well as with C- and N-terminal pHluorin constructs of WT dysferlin. After being placed in culture, samples were imaged under confocal optics at pH 7.5, then at pH 6.5 and again at pH 7.5. The ratios of the intensities at pH 6.5 to the second measurement at pH 7.5 are shown. Statistical differences were assessed by Kruskal-Wallis followed by Dunn's multiple comparison: \*statistically different from pHluorin linked to the N-terminus of WT dysferlin (pHI-WT-Dysf),  $P < 0.0001$ . [Colour figure can be viewed at wileyonlinelibrary.com]



## Ca<sup>2+</sup> signalling

Our previous results showed that voltage-induced Ca<sup>2+</sup> transients are lower in amplitude in dysferlin-null muscle fibres than in wild-type fibres (Kerr *et al.* 2013; Lukyanenko *et al.* 2017). They also showed that dysferlin reintroduced into myofibres concentrates in TT, where it stabilizes the Ca<sup>2+</sup> transient after a mild hypo-osmotic shock injury (OSI) and suppresses the generation of Ca<sup>2+</sup> waves (Lukyanenko *et al.* 2017). As most of the dysferlin variants lacking C2 domains fail to target the TT properly, we predicted that these variants would

similarly fail to replicate the effects of WT dysferlin on Ca<sup>2+</sup> signalling. When we studied myofibres expressing each of the Venus–dysferlin fusion proteins, we obtained a range of results, however (Fig. 4A).

In fibres assayed after transfection but before OSI, the amplitudes of Ca<sup>2+</sup> transients were statistically identical in fibres transfected with Venus–Dysf-WT, or with each of the dysferlin variants, with two exceptions, Dysf- $\Delta$ C2C and - $\Delta$ C2D (Figs 4A and B). In the absence of C2C, the amplitude of the Ca<sup>2+</sup> transient was reduced by 32%, whereas in the absence of C2D the reduction was ~13%.

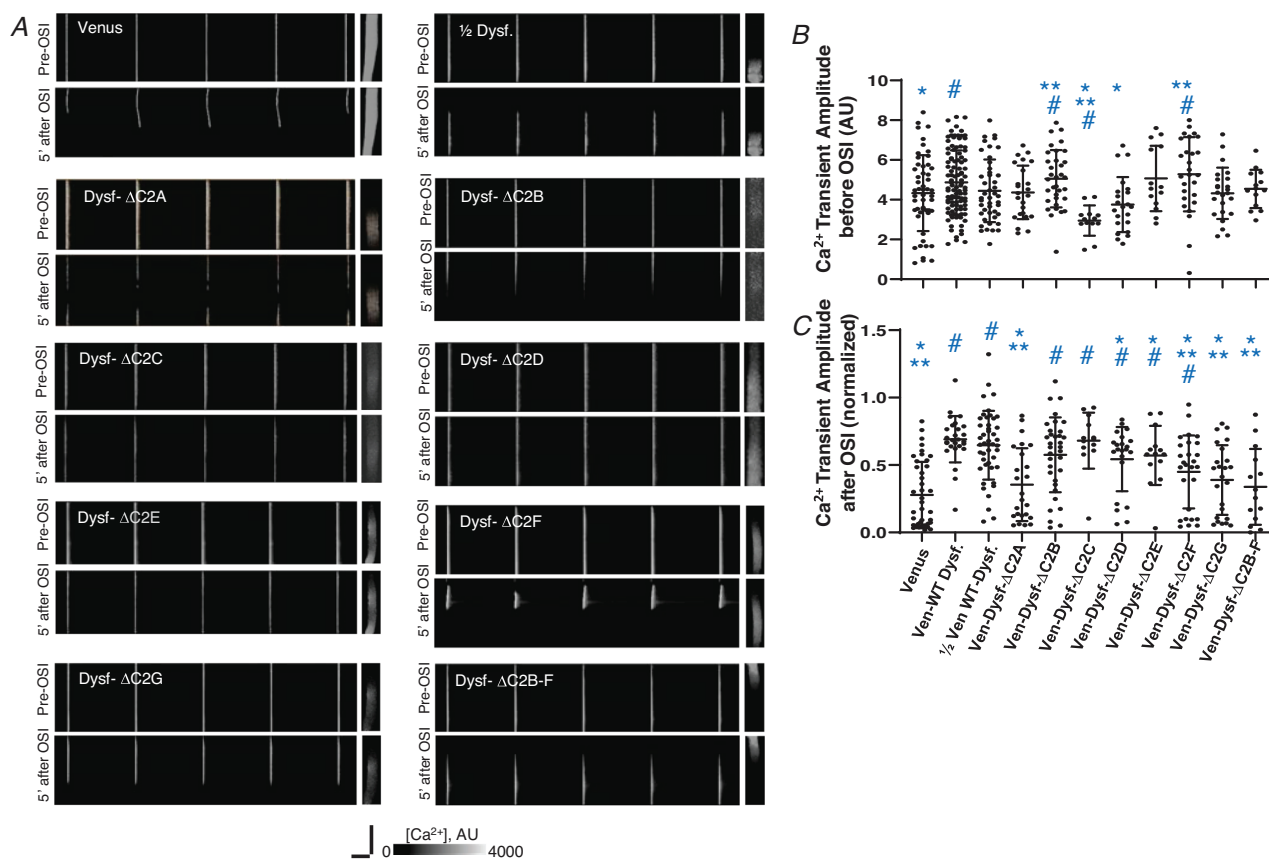


**Figure 4. Ca<sup>2+</sup> transients supported by the C2 deletion mutants before and after OSI**

A, FDB muscles were transfected and cultured as in Fig. 2, but some of the samples were transfected with 0.6  $\mu$ g instead of 1.2  $\mu$ g DNA (1/2 Dysf) and others were transfected to express Venus alone. After 24 h, they were loaded with Rhod-2AM (see Methods) and then electrically stimulated at 1 Hz, to generate the upper panels in each pair. Fibres were then subjected to a brief hypoosmotic shock (OSI) and assayed again 5 min after being returned to isotonicity, to generate the lower panels in each pair. The small fluorescence images to the right of each pair show the distribution of the Venus or Venus–dysferlin constructs for which the results are shown. B and C, quantitative values for the amplitudes of the Ca<sup>2+</sup> transients obtained before (B) and after (C) OSI. AU, arbitrary units. Statistically significant differences between each experimental construct and the three controls (Dysf, 1/2 Dysf and Venus) were calculated with Students' *t*-test and Mann–Whitney *U*-statistics, when appropriate. \*Statistically different from WT dysferlin (WT-Dysf): panel B, Venus,  $P = 0.0326$ ; Dysf- $\Delta$ C2C,  $P < 0.0001$ ; Dysf- $\Delta$ C2D,  $P = 0.0033$ ; panel C, Venus, Dysf- $\Delta$ C2C, - $\Delta$ C2F, - $\Delta$ C2G and - $\Delta$ C2B-F all show  $P < 0.0001$ ; Dysf- $\Delta$ C2D,  $P = 0.0116$ ; and Dysf- $\Delta$ C2E,  $P = 0.0202$ . \*\*Statistically different from 1/2 WT-Dysf: panel B, Dysf- $\Delta$ C2B,  $P = 0.0405$ ; Dysf- $\Delta$ C2C,  $P = 0.0018$ ; Dysf- $\Delta$ C2F,  $P = 0.0232$ ; panel C, Venus, Dysf- $\Delta$ C2A and Dysf- $\Delta$ C2G all show  $P < 0.0001$ ; Dysf- $\Delta$ C2F,  $P = 0.0013$ ; Dysf- $\Delta$ C2B-F,  $P = 0.0001$ . #Statistically different from Venus: panel B, WT-Dysf,  $P = 0.0326$ ; Dysf- $\Delta$ C2B,  $P = 0.0305$ ; Dysf- $\Delta$ C2C,  $P = 0.0019$ ; panel C, WT-Dysf, 1/2 WT-Dysf, Dysf- $\Delta$ C2B, - $\Delta$ C2C, - $\Delta$ C2D and - $\Delta$ C2E all show  $P < 0.0001$ ; Dysf- $\Delta$ C2F,  $P = 0.0098$ . [Colour figure can be viewed at [wileyonlinelibrary.com](http://wileyonlinelibrary.com)]

**Table 2. Percentage of fibres that show Ca<sup>2+</sup> waves with different dysferlin variants**

Dysferlin variant	Number of fibres	Fibres with waves	Fibres with waves (%)
None (Venus alone)	28	13	46.4
Dysferlin	19	0	0
$\frac{1}{2}$ Dysferlin	45	10	22.2
Dysf- $\Delta$ C2A	24	6	25.0
Dysf- $\Delta$ C2B	34	2	5.9
Dysf- $\Delta$ C2C	13	3	23.1
Dysf- $\Delta$ C2D	22	5	22.7
Dysf- $\Delta$ C2E	13	4	30.8
Dysf- $\Delta$ C2F	27	9	33.3
Dysf- $\Delta$ C2G	24	8	33.3
Dysf- $\Delta$ C2B-F	12	3	25.0

This suggests that these domains promote the coupling between the LTCC and RyR1 at the triad junction.

After OSI, transients in myofibres expressing Dysf- $\Delta$ C2B recovered to their initial amplitudes (Fig. 4C). Transients in fibres expressing Dysf- $\Delta$ C2C and - $\Delta$ C2D recovered to the lower amplitudes seen before OSI (Figs 4A and C). Fibres expressing Dysf- $\Delta$ C2E only partially recovered (Fig. 4C) and many of the transients induced by electrical stimulation consisted of Ca<sup>2+</sup> waves (Table 2; Fig. 5). Dysf- $\Delta$ C2A, - $\Delta$ C2F, - $\Delta$ C2G and - $\Delta$ C2B-F each failed to support significant recovery of the Ca<sup>2+</sup> transient after OSI (Fig. 4C), despite the generation of Ca<sup>2+</sup> waves either spontaneously or in response to voltage pulses (Fig. 5). Only Dysf- $\Delta$ C2B supported normal Ca<sup>2+</sup> transient amplitudes and complete recovery of transients after OSI (Fig. 4C). It also almost completely suppressed Ca<sup>2+</sup> waves (Table 2; Fig. 5). The results suggest that the most N-terminal C2 domain, C2A, and the three most C-terminal domains, C2E through C2G, are required for dysferlin to protect the Ca<sup>2+</sup> transient from the effects of OSI.

We observed that most dysferlin variants did not express in myofibres as well as Venus-Dysf-WT after identical conditions of transfection and culture. This raised the possibility that the levels of expression of the variants were not sufficient to restore activity, even if their activities were equivalent to that of WT dysferlin. We therefore studied the effects of Venus-Dysf-WT on Ca<sup>2+</sup> signalling after OSI as a function of Venus fluorescence intensity, measured in arbitrary units (see Methods). We found that even very low levels of expression of Venus-Dysf-WT, with fluorescence intensities as low as 300, generated by electroporation of lower amounts of plasmid DNA, effectively restored the amplitude of the

Ca<sup>2+</sup> transient to its initial levels, although they were not as effective in suppressing the generation of Ca<sup>2+</sup> waves (Figs 4C, 5 and 6). Specifically, halving the level of expression of Venus-Dysf-WT allowed 22% of the fibres to generate Ca<sup>2+</sup> waves with a frequency of 0.12 Hz (Fig. 6). The average fluorescence intensities for all but a few of the deletion mutants (Dysf- $\Delta$ C2C), although low, were within this range. Notably, Dysf- $\Delta$ C2B and perhaps Dysf- $\Delta$ C2A ( $P = 0.0515$ ) yielded values for the percentage of fibres showing Ca<sup>2+</sup> waves and for wave frequency similar to those we found for lower levels of WT-Dysf (average of 300 arbitrary fluorescence units), whereas deletants lacking C2E, C2F or C2G, and perhaps C2C and C2D, showed a higher percentage of fibres with waves with higher wave frequencies (Table 2; Fig. 5). Thus, the more C-terminal C2 domains of dysferlin appear to play a more important role in suppressing Ca<sup>2+</sup> waves after OSI than domains A and B.

Assuming that these results are independent of the relative spacing of the different C2 domains from each other and other regions of dysferlin, they suggest that dysferlin's activities in regulating Ca<sup>2+</sup> signalling are asymmetric, with C2A required to suppress the loss of the transient after OSI and the five most C-terminal C2 domains, C2C through C2G, playing different though potentially overlapping roles in maintaining the Ca<sup>2+</sup> transient in healthy muscle and suppressing Ca<sup>2+</sup> waves after injury.

### Sarcolemmal membrane repair

Dysferlin also plays an important role in sarcolemmal repair in skeletal muscle. We therefore studied the ability of each of the deletion mutants to mediate membrane resealing after a thermal ablation injury caused by laser illumination (Bansal *et al.* 2003; Cai *et al.* 2009a,b; McDade *et al.* 2014). As with our studies of Ca<sup>2+</sup> signalling, we introduced the dysferlin variants as Venus fusion proteins into FDB myofibres by electroporation. Ten to 14 days later, we removed the muscle and dissected out fibre bundles for further study. Notably, we did not observe obvious differences in the levels of expression of these constructs in the fibre bundles we assayed. We speculate that higher levels of expression of some of the dysferlin variants may affect the viability of myofibres when they are dissociated and placed in culture, but not in intact muscle or fibre bundles where the fibres remain in a more intact state.

When we assayed membrane repair function in fibre bundles transfected to express Venus fusion proteins of dysferlin variants lacking C2 domains, we obtained results that differed significantly from those for Ca<sup>2+</sup> signalling. In particular, all the deletants supported membrane repair to some extent (Fig. 7). When assayed in the presence

of Ca<sup>2+</sup>, which is required for dysferlin's repair activity (Bansal *et al.* 2003; Demonbreun *et al.* 2016; Gushchina *et al.* 2017; McDade *et al.* 2021), each was less active in membrane repair than WT dysferlin, with the possible exception of Dysf-ΔC2E. All of the deletants, with the possible exception of Dysf-ΔC2D, were more active in

membrane repair than untransfected A/J muscle fibres. These results indicate that each domain plays some role in membrane repair or that in the absence of a specific C2 domain other C2 domains can partially compensate during repair, even if they would not normally function in the repair response in the full length dysferlin protein.

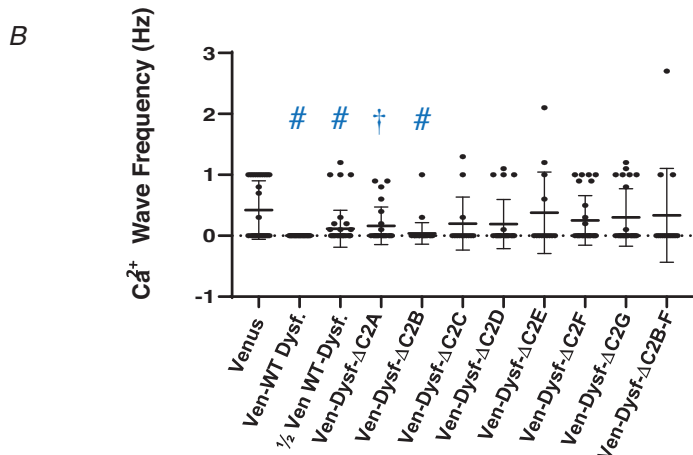
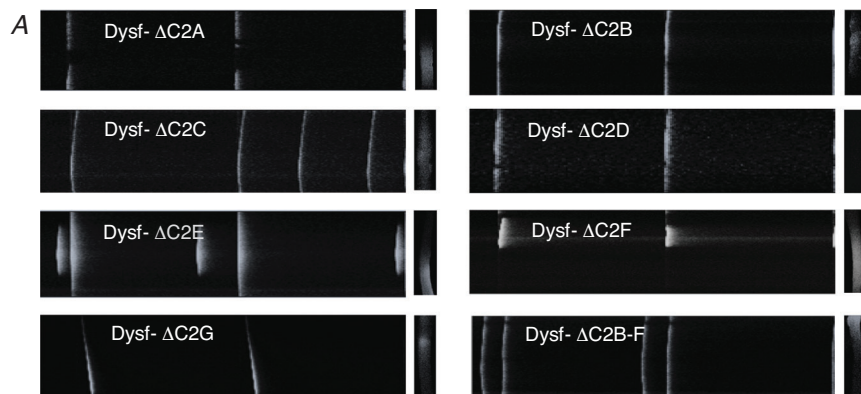


**Figure 5. Ca<sup>2+</sup> waves in fibres expressing the C2 deletion mutants**

A, as in Fig. 4A, but transients are shown in which Ca<sup>2+</sup> waves were apparent. B, frequency of Ca<sup>2+</sup> waves in transfected fibres. Statistically significant differences between each experimental construct and the Venus controls were calculated with Student's *t*-test and Mann-Whitney *U*-statistics, when appropriate. \*Statistically different from Venus: WT dysferlin,  $P < 0001$ ;  $\frac{1}{2}$  WT-Dysf,  $P = 0.0131$ ; Dysf-ΔC2B,  $P < 0001$ ; †Dysf-ΔC2A marginally different from Venus,  $P = 0.0515$ . [Colour figure can be viewed at [wileyonlinelibrary.com](http://wileyonlinelibrary.com)]

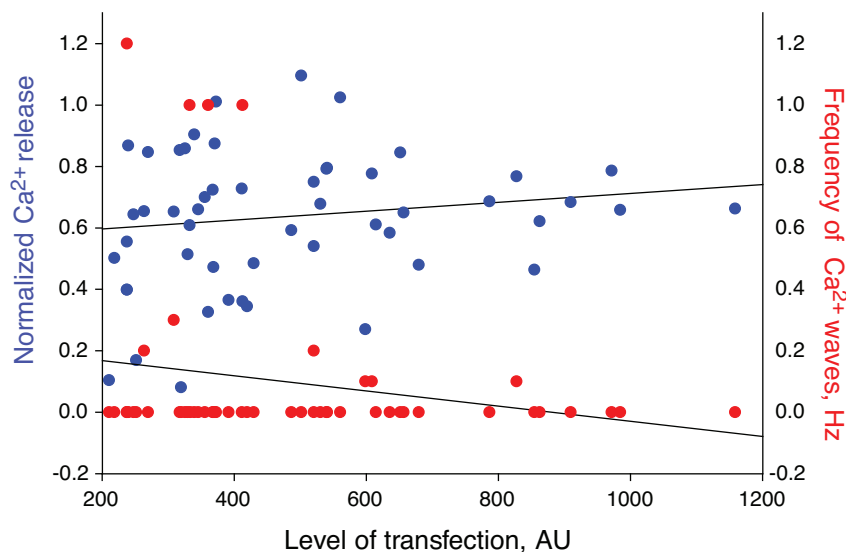


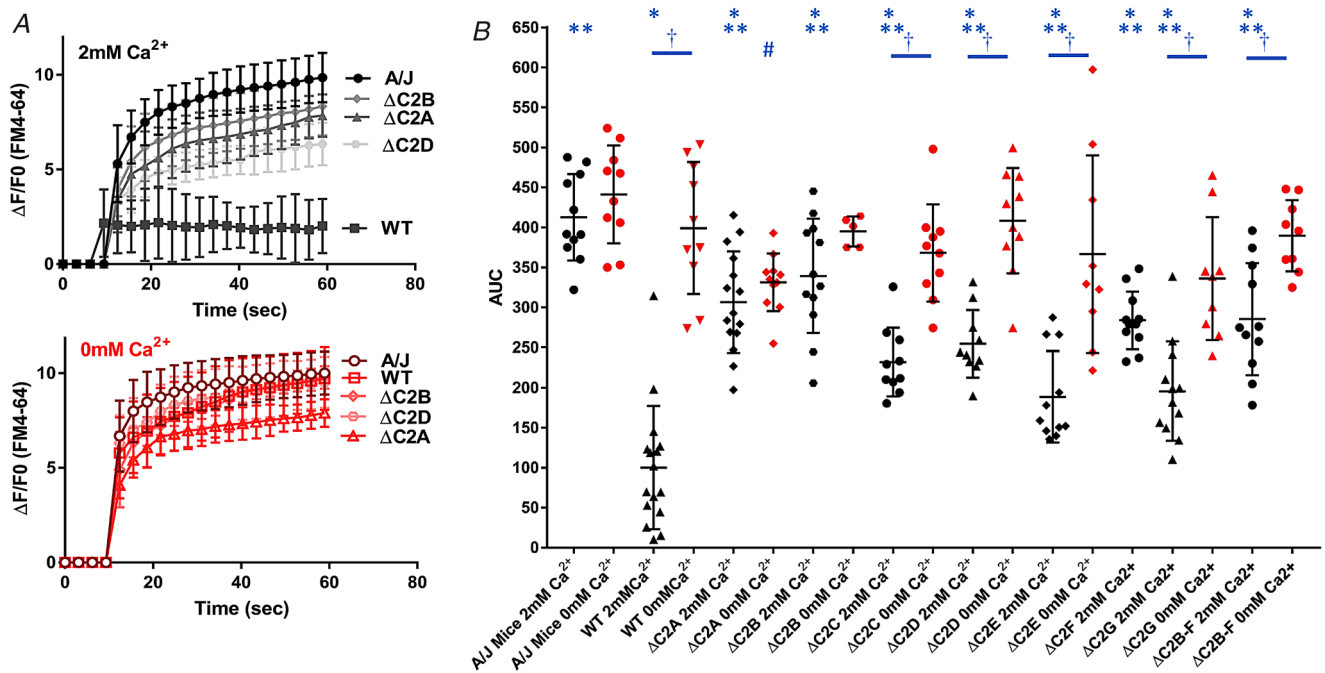
**Figure 6. Recovery from OSI and frequency of Ca<sup>2+</sup> waves as a function of WT dysferlin expression**

Fibres were transfected as in Fig. 2 with 1.2 or 0.6 μg DNA encoding Venus-WT-Dysf and then assayed after OSI as in Figs 4 and 5. Venus-WT-Dysf levels were determined in arbitrary units (AU) by measuring the intensity of the Venus fluorescence, after setting the background autofluorescence to 200 AU (see Methods).

These results suggest that, like the regulation of  $\text{Ca}^{2+}$  signalling, repair activity does not reside in a single domain alone.

The role of the C2 domains in repair was not identical, however. Statistical comparisons of the different deletants indicated that deletion of C2E and C2G each inhibited repair less than deletion of C2A or C2B, and that deletion of C2C also inhibited repair less than deletion of C2A. Thus, repair activity appeared to be distributed among dysferlin's C2 domains, though to differing extents. These results suggest that the two N-terminal domains of dysferlin, C2A and C2B, could play a more important role in repair than its more C-terminal domains. Thus, it appears that multiple C2 domains are necessary for dysferlin to function optimally in membrane repair.

We obtained further insights into the role of the C2 domains in membrane repair by assaying their activity in the absence of  $\text{Ca}^{2+}$ , which severely reduces the activity of WT dysferlin but has no effect on untransfected A/J fibres, as would be expected from previous studies in dysferlin-deficient muscle (Bansal *et al.* 2003). We found that the roles of C2 domains C, D, E and G in membrane repair were significantly promoted by  $\text{Ca}^{2+}$  (we do not have data for C2F). The role of  $\text{Ca}^{2+}$  is less clear with C2A and C2B, however. Notably, the loss of repair activity caused by the absence of  $\text{Ca}^{2+}$  is much less for each of the deletants than for WT dysferlin, further suggesting that the full complement of C2 domains and their  $\text{Ca}^{2+}$  binding activity is necessary for optimal membrane repair. The differences among the activities of the C2 domains



noted above, as well as with full length dysferlin, were eliminated in the absence of extracellular  $\text{Ca}^{2+}$ , suggesting that they were specific to the  $\text{Ca}^{2+}$  binding activities of these domains.

Assuming that these results are independent of the relative spacing of the different C2 domains from each other and other regions of dysferlin, they suggest that dysferlin's activities in membrane repair are also asymmetrically distributed, with the two N-terminal C2 domains and the five C-terminal C2 domains playing different but possibly reinforcing roles. While optimal membrane repair seems to require the full complement of C2 domains, the presence of any of these C2 domains appears to be able partially to restore the sarcolemmal repair function of the dysferlin protein. Notably, comparison to our results on  $\text{Ca}^{2+}$  signalling, above, suggests that dysferlin's C2 domains play different roles in  $\text{Ca}^{2+}$  signalling and sarcolemmal membrane repair.

## Discussion

Dysferlin in skeletal muscle was first proposed to mediate repair of the sarcolemma after injury (Bansal *et al.* 2003; Bansal & Campbell, 2004; Ho *et al.* 2004; Glover & Brown, 2007; Han & Campbell, 2007), but whether this is its sole function in muscle has been in some doubt since we reported that dysferlin concentrates primarily in the TT of skeletal muscle, where it stabilizes  $\text{Ca}^{2+}$  signalling after injury (Kerr *et al.* 2013, 2014; Lukyanenko *et al.* 2017). Specifically, we found that a mild hypo-osmotic shock injury of dysferlin-null myofibres caused the mechanism of  $\text{Ca}^{2+}$  release to change from voltage-induced to  $\text{Ca}^{2+}$ -induced, characterized by the appearance of spontaneous  $\text{Ca}^{2+}$  waves and waves triggered initially by voltage pulses. We suggested that CICR dominates the  $\text{Ca}^{2+}$  release mechanism in dysferlin-null myofibres following injury, and that, in addition to its role in membrane repair, dysferlin stabilizes the voltage-dependent mechanisms responsible for normal voltage-induced  $\text{Ca}^{2+}$  release. Roles for dysferlin in membrane repair and  $\text{Ca}^{2+}$  signalling need not be mutually exclusive or even completely distinct, however, as  $\text{Ca}^{2+}$  plays a key role in the membrane repair mechanism (Bansal *et al.* 2003; Demonbreun *et al.* 2016; Gushchina *et al.* 2017; McDade *et al.* 2021). Indeed, given its large size (237 kDa) and its dozen or so different structural domains, dysferlin could in principle serve several different functions in skeletal muscle or in other cell types. Here we tested the hypothesis that defects in  $\text{Ca}^{2+}$  signalling are the primary cause of pathology in dysferlin-null muscle, and that defects in sarcolemmal membrane repair are secondary. Our experiments studied variants of dysferlin that lack one or more C2 domains, with the prediction that any domain

deletant that compromised the stabilization of  $\text{Ca}^{2+}$  signalling would also inhibit membrane repair. Contrary to our hypothesis, our results indicate that dysferlin's C2 domains play different roles in  $\text{Ca}^{2+}$  signalling and membrane repair and suggest that changes in either or both processes can lead to dysferlinopathy.

Several different  $\text{Ca}^{2+}$  signalling phenotypes are apparent in dysferlin-null A/J myofibres transfected to express dysferlin lacking one of its C2 domains or its five middle C2 domains, B through F (Fig. 8). We evaluated the effects of these variants by comparing them to the effects we observed in the complete absence of dysferlin, i.e. in A/J fibres transfected to express Venus alone. The initial amplitude of the  $\text{Ca}^{2+}$  transients in this preparation is  $\sim 15\%$  lower than control myofibres or the regions of fibres expressing wild-type dysferlin introduced by electroporation, but it is statistically indistinguishable from regions of transfected fibres that fail to express exogenous dysferlin (Lukyanenko *et al.* 2017). After OSI, however, the  $\text{Ca}^{2+}$  transient of fibres expressing only Venus decreases in amplitude by 60–70% and many fibres (46%) show evidence of CICR, in the form of  $\text{Ca}^{2+}$  waves (see also (Kerr *et al.* 2013; Lukyanenko *et al.* 2017). Unlike transfection with Venus, transfection with wild-type dysferlin (Venus–Dysf-WT) supports the complete recovery of the amplitude of the  $\text{Ca}^{2+}$  transient and completely suppresses  $\text{Ca}^{2+}$  waves, but only in the regions of the fibres where dysferlin is expressed (Lukyanenko *et al.* 2017); regions failing to express exogenous dysferlin behave like fibres transfected with Venus alone. Thus, WT dysferlin protects the transient against the consequences of damage caused by OSI and completely suppresses waves, indicative of CICR. In dysferlin's complete absence, CICR is not always as efficient as voltage-induced  $\text{Ca}^{2+}$  release, as the amplitudes of many  $\text{Ca}^{2+}$  waves after OSI remain low compared to the amplitudes of transients induced initially by voltage pulses.

Our results also show that in the presence of reduced levels of WT dysferlin the amplitude of the  $\text{Ca}^{2+}$  transient is restored after OSI, but  $\sim 20\%$  of the fibres show low frequency  $\text{Ca}^{2+}$  waves. Because they are expressed at low levels in transfected and cultured A/J myofibres, the individual C2 domain deletion mutants should be compared to Dysf-WT expressed at comparably reduced levels. When this condition is met, Dysf- $\Delta$ C2B has effects on  $\text{Ca}^{2+}$  signalling similar to the effects of expressing WT dysferlin, suggesting that the C2B domain does not play a significant role in the regulation of excitation–contraction coupling in otherwise dysferlin-null myofibres. By contrast, Dysf- $\Delta$ C2A is almost as effective as Dysf-WT in suppressing  $\text{Ca}^{2+}$  waves but it fails to protect the amplitude of the  $\text{Ca}^{2+}$  transient against loss following OSI, suggesting that it contributes to stabilizing the LTCC-RyR1 couplon responsible for  $\text{Ca}^{2+}$  release.

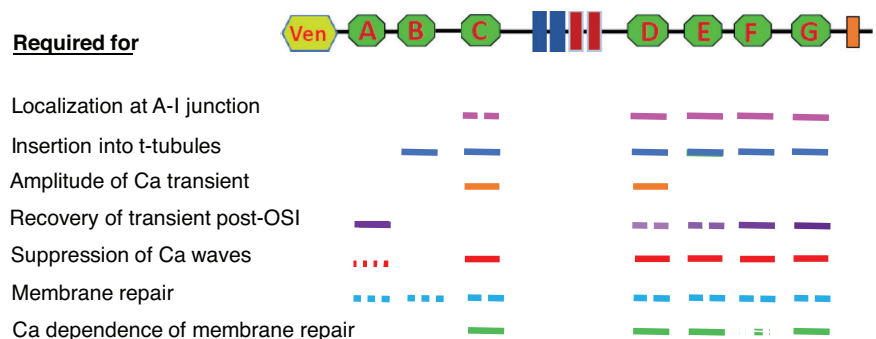
Deletion of the other C2 domains individually or domains B–F together effects greater changes in Ca<sup>2+</sup> signalling. Dysf-ΔC2C and -ΔC2D reduce the amplitude of the Ca<sup>2+</sup> transient even before OSI, and, although Dysf-ΔC2C restores the amplitude to its original low level after OSI, it appears less effective than low levels of Dysf-WT in suppressing Ca<sup>2+</sup> waves (Fig. 5). Dysf-ΔC2D, -ΔC2E, -ΔC2F, -ΔC2G and -ΔC2B–F all fail to restore the amplitude of the Ca<sup>2+</sup> transient after OSI and fail to suppress Ca<sup>2+</sup> waves, although to differing extents. Notably, there appears to be a gradient in efficacy from C2D through C2G, suggesting that the more C-terminal C2 domains play a greater role. Additional experiments will be needed to assess this more thoroughly. Nevertheless, our data suggest that the C2 domains in the C-terminal half of dysferlin are required to stabilize the Ca<sup>2+</sup> transient and suppress CICR in A/J myofibres subjected to OSI.

Contrary to our original prediction, the roles of the C2 domains in sarcolemmal membrane repair appear to be distinct. In laser-mediated wounding assays, the absence of C2A and C2B results in significantly compromised membrane repair, whereas removal of any of the more C-terminal C2 domains allows membrane repair to proceed, although not as efficiently as it does in WT muscle. Our data suggest that C2C, C2D, C2E, C2F and C2G contribute almost equally well to sarcolemmal membrane repair and in a Ca<sup>2+</sup>-dependent manner, typical of the WT protein. Thus, dysferlin appears to show considerable polarization in its structure–function relationships, with stabilization of Ca<sup>2+</sup> signalling concentrated in the C2A domain and membrane repair activity dependent on the two N-terminal C2 domains, with significant contributions of domains C2C to C2G for optimal repair. It will be of considerable interest to learn how this distribution of activities correlates with dysferlin's ability to associate with other proteins associated with membrane repair, such as annexins, caveolin 3 and TRIM72/MG53, and how these in turn influence the activities of the variants we have characterized here.

Our results further suggest that there is no clear relationship between subcellular localization of the dysferlin variants and their roles in either sarcolemmal membrane repair or Ca<sup>2+</sup> signalling. For example, deletion of C2A does not inhibit trafficking of the mutant protein to the TT, but it inhibits membrane repair and recovery of the Ca<sup>2+</sup> transient after injury. Thus, targeting to the TT is not sufficient for dysferlin to be functional in either supporting normal Ca<sup>2+</sup> signalling or membrane repair. Likewise, deletants lacking C2E, C2F or C2G support membrane repair although they concentrate in what is likely to be a compartment of the ER rather than in TT. Perhaps most strikingly, Dysf-ΔC2B concentrates in punctate structures at the level of A–I junctions but it fails to accumulate in TT, as assayed by our pHLuorin method. Nevertheless, it fully stabilizes Ca<sup>2+</sup> signalling, when compared to comparable levels of Dysf-WT. One possible explanation of this result is that our pHLuorin methods fail to detect small but significant amounts of the dysferlin chimera oriented like the wild-type pHLuorin protein, and that these reduced levels of dysferlin in the TT are sufficient to support normal Ca<sup>2+</sup> signalling. Another is that the Dysf-ΔC2B construct only exposes its C-terminal pHLuorin moiety to the lumen of the TT after hypoosmotic shock. Although we are testing these and other possibilities, the simplest interpretation is that dysferlin needs to concentrate *near* but not *in* TT in order to regulate Ca<sup>2+</sup> release.

Our results indicate that dysferlin's several activities are distributed along the length of the molecule in distinct patterns, which we summarize in Fig. 8. The ability of the individual C2 domains of dysferlin to bind Ca<sup>2+</sup> and phospholipid vesicles with different apparent affinities (Abdullah *et al.* 2014) is consistent with the idea that dysferlin's C2 domains have distinct activities. 'Nanodysferlins' (small versions of the dysferlin molecule lacking different C2 domains) that can be expressed in muscle by adeno-associated viruses are now being tested as possible gene therapies for dysferlinopathies (e.g. Llanga *et al.* 2017). Given the roles played by dysferlin's C2 domains, it will likely require considerable ingenuity

**Figure 8. Summary of the results of our assays of the C2 deletion mutants**  
Continuous lines indicate that the domain is strongly associated with that function. Dashed lines with longer or shorter dashes indicate weak and even weaker associations, respectively. The dotted line indicates a difference that is only marginally significant. The single green dot under C2F indicates that this was not assayed.



to generate a nanodysferlin that retains the activities required to maintain healthy muscle. These studies do, however, point towards key domains that are necessary to support dysferlin's function in muscle and thus should provide insight for future developments of therapeutic approaches.

Although our results do not indicate any coordination of activities between C2 domains, we cannot rule out the possibility that deletion of any given domain alters the positioning of the other domains with respect to each other, thereby disrupting activities that require their proper alignment in the wild-type protein. Additional studies of dysferlin variants carrying pathogenic point mutations or lacking different combinations of the C2 domains may address this possibility. Furthermore, since we made our deletions the boundaries of individual C2 domains, predicted by AlphaFold2 and RoseTTA-fold, have likely shifted. Despite this, the sequences we have deleted completely disrupt each of the C2 domains of dysferlin (R. B. Sutton, personal communication). Once these structural boundaries are set more firmly, we will be using a more finely tuned approach to confirm and extend our studies.

## References

- Abdullah N, Padmanarayana M, Marty NJ & Johnson CP (2014). Quantitation of the calcium and membrane binding properties of the C2 domains of dysferlin. *Biophys J* **106**, 382–389.
- Amato AA & Brown RH Jr (2011). Dysferlinopathies. *Handb Clin Neurol* **101**, 111–118.
- Ampong BN, Imamura M, Matsumiya T, Yoshida M & Takeda S (2005). Intracellular localization of dysferlin and its association with the dihydropyridine receptor. *Acta Myol* **24**, 134–144.
- Anderson LV, Moss JA, Young C, Cullen MJ, Walsh J, Johnson MA, Bashir R, Britton S, Keers S, Argov Z, Mahjneh I, Fougousse F, Beckman JS & Bushby KM (1999). Dysferlin is a plasma membrane protein and is expressed early in human development. *Hum Mol Genet* **8**, 855–861.
- Bansal D & Campbell KP (2004). Dysferlin and the plasma membrane repair in muscular dystrophy. *Trends Cell Biol* **14**, 206–213.
- Bansal D, Miyake K, Vogel SS, Groh S, Chen CC, Williamson R, McNeil PL & Campbell KP (2003). Defective membrane repair in dysferlin-deficient muscular dystrophy. *Nature* **423**, 168–172.
- Cai C, Masumiya H, Weisleder N, Matsuda N, Nishi M, Hwang M, Ko JK, Lin P, Thornton A, Zhao X, Pan Z, Komazaki S, Brotto M, Takeshima H & Ma J (2009a). MG53 nucleates assembly of cell membrane repair machinery. *Nat Cell Biol* **11**, 56–64.
- Cai C, Weisleder N, Ko JK, Komazaki S, Sunada Y, Nishi M, Takeshima H & Ma J (2009b). Membrane repair defects in muscular dystrophy are linked to altered interaction between MG53, caveolin-3, and dysferlin. *J Biol Chem* **284**, 15894–15902.
- Carmeille R, Bouvet F, Tan S, Croissant C, Gounou C, Mamchaoui K, Mouly V, Brisson AR & Bouter A (2016). Membrane repair of human skeletal muscle cells requires annexin-A5. *Biochim Biophys Acta* **1863**, 2267–2279.
- Cenacchi G, Fanin M, Di Giorgi LB & Angelini C (2005). Ultrastructural changes in dysferlinopathy support defective membrane repair mechanism. *J Clin Pathol* **58**, 190–195.
- Codding SJ, Marty N, Abdullah N & Johnson CP (2016). Dysferlin binds SNAREs (soluble N-ethylmaleimide-sensitive factor (NSF) attachment protein receptors) and stimulates membrane fusion in a calcium-sensitive manner. *J Biol Chem* **291**, 14575–14584.
- Davenport NR & Bement WM (2016). Cell repair: revisiting the patch hypothesis. *Commun Integr Biol* **9**, e1253643.
- Davis DB, Doherty KR, Delmonte AJ & McNally EM (2002). Calcium-sensitive phospholipid binding properties of normal and mutant ferlin C2 domains. *J Biol Chem* **277**, 22883–22888.
- Demonbreun AR, Quattrocchi M, Barefield DY, Allen MV, Swanson KE & McNally EM (2016). An actin-dependent annexin complex mediates plasma membrane repair in muscle. *J Cell Biol* **213**, 705–718.
- de Morrée A, Hensbergen PJ, van Haagen HH, Dragan I, Deelder AM, 't Hoen PA, Frants RR & van der Maarel SM (2010). Proteomic analysis of the dysferlin protein complex unveils its importance for sarcolemmal maintenance and integrity. *PLoS One* **5**, e13854.
- DiFranco M, Quinonez M, Capote J & Vergara J (2009). DNA transfection of mammalian skeletal muscles using in vivo electroporation. *J Vis Exp* **19**, 1520.
- Endo M (2009). Calcium-induced calcium release in skeletal muscle. *Physiol Rev* **89**, 1153–1176.
- Fuson K, Rice A, Mahling R, Snow A, Nayak K, Shanbhogue P, Meyer AG, Redpath GM, Hinderliter A, Cooper ST & Sutton RB (2014). Alternate splicing of dysferlin C2A confers Ca<sup>2+</sup>-dependent and Ca<sup>2+</sup>-independent binding for membrane repair. *Structure* **22**, 104–115.
- Glover L & Brown RH Jr (2007). Dysferlin in membrane trafficking and patch repair. *Traffic* **8**, 785–794.
- Golbek TW, Otto SC, Roeters SJ, Weidner T, Johnson CP & Baio JE (2021). Direct evidence that mutations within dysferlin's C2A domain inhibit lipid clustering. *J Phys Chem B* **125**, 148–157.
- Gushchina LV, Bhattacharya S, McElhanon KE, Choi JH, Manring H, Beck EX, Alloush J & Weisleder N (2017). Treatment with recombinant human MG53 protein increases membrane integrity in a mouse model of limb girdle muscular dystrophy 2B. *Mol Ther* **25**, 2360–2371.
- Han R & Campbell KP (2007). Dysferlin and muscle membrane repair. *Curr Opin Cell Biol* **19**, 409–416.
- Han WQ, Xia M, Xu M, Boini KM, Ritter JK, Li NJ & Li PL (2012). Lysosome fusion to the cell membrane is mediated by the dysferlin C2A domain in coronary arterial endothelial cells. *J Cell Sci* **125**, 1225–1234.
- Hernández-Deviez DJ, Martin S, Laval SH, Lo HP, Cooper ST, North KN, Bushby K & Parton RG (2006). Aberrant dysferlin trafficking in cells lacking caveolin or expressing dystrophy mutants of caveolin-3. *Hum Mol Genet* **15**, 129–142.

- Ho M, Post CM, Donahue LR, Lidov HG, Bronson RT, Goolsby H, Watkins SC, Cox GA & Brown RH Jr (2004). Disruption of muscle membrane and phenotype divergence in two novel mouse models of dysferlin deficiency. *Hum Mol Gen* **13**, 1999–2010.
- Huang YC, Laval SH, van Remoortere A, Baudier J, Benaud C, Anderson LVB, Straub V, Deelder A, Frants RR, den Dunnen JT, Bushby K & van der Maarel SM (2007). AHNAK, a novel component of the dysferlin protein complex, redistributes to the cytoplasm with dysferlin during skeletal muscle regeneration. *FASEB J* **21**, 731–742.
- Jethwaney D, Islam MR, Leidal KG, de Bernabe DB, Campbell KP, Nauseef WM & Gibson BW (2007). Proteomic analysis of plasma membrane and secretory vesicles from human neutrophils. *Proteome Sci* **5**, 12.
- Kerr JP, Ward CW & Bloch RJ (2014). Dysferlin at transverse tubules regulates  $Ca^{2+}$  homeostasis in skeletal muscle. *Front Physiol* **5**, 89.
- Kerr JP, Ziman AP, Mueller AL, Muriel JM, Kleinhans-Welte E, Gumerson JD, Vogel SS, Ward CW, Roche JA & Bloch RJ (2013). Dysferlin stabilizes stress-induced  $Ca^{2+}$  signaling in the transverse tubule membrane. *Proc Natl Acad Sci U S A* **110**, 20831–20836.
- Klinge L, Laval S, Keers S, Haldane F, Straub V, Barresi R & Bushby K (2007). From T-tubule to sarcolemma: damage-induced dysferlin translocation in early myogenesis. *FASEB J* **21**, 1768–1776.
- Lek A, Evesson FJ, Sutton RB, North KN & Cooper ST (2012). Ferlins: regulators of vesicle fusion for auditory neurotransmission, receptor trafficking and membrane repair. *Traffic* **13**, 185–194.
- Lennon NJ, Kho A, Bacskai BJ, Perlmutter SL, Hyman BT & Brown RH Jr (2003). Dysferlin interacts with annexins A1 and A2 and mediates sarcolemmal wound-healing. *J Biol Chem* **278**, 50466–50473.
- Llanga T, Nagy N, Conatser L, Dial C, Sutton RB & Hirsch ML (2017). Structure-based designed nano-dysferlin significantly improves dysferlinopathy in BLA/J mice. *Mol Ther* **25**, 2150–2162.
- Lukyanenko V, Muriel JM & Bloch RJ (2017). Coupling of excitation to  $Ca^{2+}$  release is modulated by dysferlin. *J Physiol* **595**, 5191–5207.
- Marty NJ, Holman CL, Abdullah N & Johnson CP (2013). The C2 domains of otoferlin, dysferlin, and myoferlin alter the packing of lipid bilayers. *Biochem* **52**, 5585–5592.
- Matsuda C, Hayashi YK, Ogawa M, Aoki M, Murayama K, Nishino I, Nonaka I, Arahata K & Brown RH Jr (2001). The sarcolemmal proteins dysferlin and caveolin-3 interact in skeletal muscle. *Hum Mol Genet* **10**, 1761–1766.
- Matsuda C, Miyake K, Kameyama K, Keduka E, Takeshima H, Imamura T, Araki N, Nishino I & Hayashi Y (2012). The C2A domain in dysferlin is important for association with MG53 (TRIM72). *PLoS Curr* **4**, e5035add8caff4.
- McDade JR, Archambeau A & Michele DE (2014). Rapid actin-cytoskeleton-dependent recruitment of plasma membrane-derived dysferlin at wounds is critical for muscle membrane repair. *FASEB J* **28**, 3660–3670.
- McDade JR, Naylor MT & Michele DE (2021). Sarcolemma wounding activates dynamin-dependent endocytosis in striated muscle. *FEBS J* **288**, 160–174.
- McNeil PL, Vogel SS, Miyake K & Terasaki M (2000). Patching plasma membrane disruptions with cytoplasmic membrane. *J Cell Sci* **113**, 1891–1902.
- Patel NJ, Van Dyke KW & Espinoza LR (2017). Limb-girdle muscular dystrophy 2B and miyoshi presentations of dysferlinopathy. *Am J Med Sci* **353**, 484–491.
- Piccolo F, Moore SA, Ford GC & Campbell KP (2000). Intracellular accumulation and reduced sarcolemmal expression of dysferlin in limb-girdle muscular dystrophies. *Ann Neurol* **48**, 902–912.
- Ríos E (2018). Calcium-induced release of calcium in muscle: 50 years of work and the emerging consensus. *J Gen Physiol* **150**, 521–537.
- Roche JA, Lovering RM & Bloch RJ (2008). Impaired recovery of dysferlin-null skeletal muscle after contraction-induced injury in vivo. *NeuroReport* **19**, 1579–1584.
- Roche JA, Lovering RM, Roche R, Ru L, Reed PW & Bloch RJ (2010). Extensive mononuclear infiltration and myogenesis characterize the recovery of dysferlin-null skeletal muscle from contraction-induced injuries. *Am J Physiol Cell Physiol* **298**, C298–C312.
- Roche JA, Ru LW, O'Neill AM, Resneck WG, Lovering RM & Bloch RJ (2011). Unmasking potential intracellular roles for dysferlin through improved immunolabeling methods. *J Histochem Cytochem* **59**, 964–975.
- Sakellariou P, O'Neill A, Mueller AL, Stadler G, Wright WE, Roche JA & Bloch RJ (2016). Neuromuscular electrical stimulation promotes development in mice of mature human muscle from immortalized human myoblasts. *Skelet Muscle* **6**, 4.
- Selcen D, Stilling G & Engel AG (2001). The earliest pathologic alterations in dysferlinopathy. *Neurol* **56**, 1472–1481.
- Therrien C, Di Fulvio S, Pickles S & Sinnreich M (2009). Characterization of lipid binding specificities of dysferlin C2 domains reveals novel interactions with phosphoinositides. *Biochem* **48**, 2377–2384.
- Urtizberea JA, Bassez G, Leturcq F, Nguyen K, Krahn M & Levy N (2008). Dysferlinopathies. *Neurol India* **56**, 289–297.
- Waddell LB, Lemckert FA, Zheng XF, Tran J, Evesson FJ, Hawkes JM, Lek A, Street NE, Lin P, Clarke NF, Landstrom AP, Ackerman MJ, Weisleder N, Ma J, North KN & Cooper ST (2011). Dysferlin, annexin A1, and mitsugumin 53 are upregulated in muscular dystrophy and localize to longitudinal tubules of the T-system with stretch. *J Neuro-pathol Exper Neurol* **70**, 302–313.
- Wang Y, Tadayon R, Santamaria L, Mercier P, Forristal CJ & Shaw GS (2021). Calcium binds and rigidifies the dysferlin C2A domain in a tightly coupled manner. *Biochem J* **478**, 197–215.
- Weisleder N, Takeshima H & Ma J (2009). Mitsugumin 53 (MG53) facilitates vesicle trafficking in striated muscle to contribute to cell membrane repair. *Commun Integr Biol* **2**, 225–226.
- Weisleder N, Takizawa N, Lin P, Wang X, Cao C, Zhang Y, Tan T, Ferrante C, Zhu H, Chen PJ, Yan R, Sterling M, Zhao X, Hwang M, Takeshima M, Cai C, Cheng H, Takeshima H, Xiao RP & Ma J (2012). Recombinant MG53 protein modulates therapeutic cell membrane repair in treatment of muscular dystrophy. *Sci Transl Med* **4**, 139ra185.

Zhao X, Moloughney JG, Zhang S, Komzaki S & Weisleder N (2012). Orai1 mediates exacerbated  $\text{Ca}^{2+}$  entry in dystrophic skeletal muscle. *PLoS One* 7, e49862.

## Additional information

### Data availability statement

The data that support the findings of this study are available from the corresponding authors, NW and RJB, upon request.

### Competing interests

None of the authors has any conflicts of interest or competing interests.

### Author contributions

Conception or design of the work: J.M., V.L., T.K., S.B., D.G., N.W., R.B.; Acquisition or analysis or interpretation of data for the work: J.M., V.L., T.K., S.B., D.G., N.W., R.B. Drafting the work or revising it critically for important intellectual content: N.W., R.B. All authors have read and approved the final version of this manuscript and agree to be accountable for all aspects of the work in ensuring that questions related to the accuracy or integrity of any part of the work are appropriately investigated and resolved. All persons designated as authors qualify for authorship, and all those who qualify for authorship are listed.

### Funding

S.B. was the recipient of an Ohio State/Nationwide Children's Hospital Center for Muscle Health and Neuromuscular Disorders Postdoctoral Fellowship. This work was supported by grants from the Jain Foundation and the National Institutes of Health to N.W. (RO1 AG056504) and R.J.B. (2 RO1 AR064268), by funds generously provided to R.J.B. from the Department of Physiology, University of Maryland School of Medicine, and by resources from the Campus Microscopy and Imaging Facility (CMIF) and the OSU Comprehensive Cancer Center (OSUCCC) Microscopy Shared Resource (MSR), The Ohio State University.

### Acknowledgements

R.J.B. thanks Andrea O'Neill for assistance with statistical analyses and Roger B. Sutton (Texas Tech University Health Sciences Center, Lubbock TX) for useful discussions.

### Keywords

$\text{Ca}^{2+}$  transient,  $\text{Ca}^{2+}$  waves, CICR, EC coupling, injury, membrane repair, sarcolemma, transverse tubule

## Supporting information

Additional supporting information can be found online in the Supporting Information section at the end of the HTML view of the article. Supporting information files available:

### Peer Review History Statistical Summary Document